

# Microinjection of the Catalytic Fragment of Myosin Light Chain Kinase into Dividing Cells: Effects on Mitosis and Cytokinesis

Douglas J. Fishkind, Long-guang Cao, and Yu-li Wang

Cell Biology Group, Worcester Foundation for Experimental Biology, Shrewsbury, Massachusetts 01545

**Abstract.** Myosin light chain kinase (MLCK) is thought to regulate the contractile activity in smooth and non-muscle cells, and may play an important role in controlling the reorganization of the actin-myosin cytoskeleton during cell division. To test this hypothesis we have microinjected the 61-kD catalytic fragment of MLCK into mitotic cells, and examined the effects of unregulated MLCK activity on cell division. The microinjection of active 61 kD causes both a significant delay in the transit time from nuclear envelope breakdown to anaphase onset, and an increase in motile surface activity during and after metaphase. Control experiments with intact MLCK or with inactive catalytic fragment suggest that these effects are specifically in-

duced by the unregulated myosin light chain kinase activity. Immunofluorescence analysis suggests that delays in mitosis are coupled to disruptions of spindle structures, while increased surface motility may be related to changes in the organization of actin and myosin at the cell cortex. Most importantly, despite the expression of strong phenotypes, 61 kD-injected cells still form functional cleavage furrows that progress through cytokinesis at rates identical to those of control cells. Together, these results suggest that the activity of MLCK can affect mitosis and cortical activities, however additional control mechanisms are likely involved in the regulation of cytokinesis.

**A**CTIN and myosin undergo precisely regulated reorganizations in cultured animal cells during mitosis, including the disassembly of stress fibers during prophase/prometaphase (Sanger et al., 1989), the increase in cortical association during metaphase/anaphase (Kitanishi-Yumura and Fukui, 1989; Cao and Wang, 1990b), and the redistribution into the equatorial region during cytokinesis (see Mabuchi, 1986; Salmon, 1989 for reviews). Although the exact roles of these activities are unclear, it is generally agreed that the interaction of cortical actin and myosin II generates the contractile force for cytokinesis (Mabuchi, 1986; Salmon, 1989 for reviews). The involvement of myosin II in cytokinesis, in particular, is supported by a large body of evidence, including the presence of myosin in the equatorial region during cell cleavage (Fujiwara and Pollard, 1976, 1978; Aubin et al., 1979; Nunnally et al., 1980; Yumura et al., 1984; Maupin and Pollard, 1986; Schroeder, 1987; Sanger et al., 1989), and the ability of microinjected antibodies against myosin to inhibit cytokinesis (Mabuchi and Okuno, 1977; Kiehart et al., 1982; Zurek et al., 1990). Moreover, inhibition of cytokinesis has also been observed with genetically manipulated cells lacking myosin II (Knecht and Loomis, 1987) or expressing defective myosin II molecules (De Lozanne and Spudich, 1987).

While the requirement of myosin II for cytokinesis is well established, important questions remain as to how the inter-

actions between actin and myosin II are spatially and temporally regulated in dividing cells. For both smooth- and non-muscle cells, one of the best-characterized mechanisms for the regulation of actin-myosin interactions is through phosphorylation of the 20-kD regulatory myosin light chain (MLC<sub>20</sub>) by the Ca<sup>2+</sup>/calmodulin-dependent enzyme myosin light chain kinase (MLCK)<sup>1</sup> (Kamm and Stull, 1985; Sellers and Adelstein, 1987). This enzyme catalyzes the specific phosphorylation of MLC<sub>20</sub> on serine 19, which in turn stimulates the actin-activated MgATPase of myosin, the assembly of myosin filaments under physiological conditions, and the ability of myosin to generate force (Sellers and Adelstein, 1987; Warrick and Spudich, 1987; Korn and Hammer, 1988). Thus, it has been proposed that differences in the phosphorylation state of MLC<sub>20</sub>, may control the organization and contractile activity of myosin during cell division (Pollard et al., 1990; Mabuchi, 1990).

One way to test this hypothesis is to overcome the dependence of MLCK on Ca<sup>2+</sup>/calmodulin, and ask whether cell division is influenced by the unregulated catalytic activity of the kinase. Ikebe and colleagues have previously mapped the domain structure of MLCK and characterized a 61-kD tryptic fragment that possesses the catalytic activity even in the

1. *Abbreviations used in this paper:* MLCK, myosin light chain kinase; NEB, nuclear envelope breakdown; NRK, normal rat kidney.

absence of the  $\text{Ca}^{2+}$ /calmodulin complex (Ikebe et al., 1987a, 1989). Microinjection of this fragment into smooth muscle cells induces contraction without the requirement for the release of  $\text{Ca}^{2+}$  (Itoh et al., 1989). In this study, we have prepared this catalytic fragment and microinjected it into mitotic normal rat kidney (NRK) cells soon after nuclear envelope breakdown (NEB). Interestingly, the microinjection caused a significant delay in mitosis during prometaphase/metaphase and an increase in surface activities during metaphase, anaphase, and telophase. However, after the onset of anaphase, the cleavage furrow formed at the proper time and location in the cell, at a rate identical to that of controls. We conclude that while the regulation of MLCK activity can affect mitosis and cortical activities, the control of cytokinesis probably involves additional factors.

## Materials and Methods

### Preparation of MLCK and its Catalytic Fragment

MLCK was prepared from turkey gizzards by the method of Walsh et al. (1983), as modified by Ikebe et al. (1987a). After phosphocellulose chromatography, MLCK was further purified by calmodulin-affinity chromatography as described by Adelstein and Klee (1982) and dialyzed into a storage buffer of 50 mM KCl, 30 mM Tris-HCl, 0.5 mM DTT, pH 7.5.

The catalytic fragment of MLCK was prepared by limited proteolysis of MLCK in the presence of  $\text{Ca}^{2+}$  and calmodulin as detailed by Ikebe et al. (1987a, 1989). Briefly, MLCK (0.5 mg/ml) in the storage buffer containing 0.2 mM  $\text{CaCl}_2$  was proteolyzed with trypsin (1:100, wt/wt) in the presence of 0.2 mg/ml calmodulin for 7.5 min at 25°C. The reaction was terminated by the addition of a twofold (wt/wt) excess of soybean trypsin inhibitor over trypsin, and the solution was subjected to anion-exchange chromatography on either a DEAE-Sepharose Fast Flow exchanger (Pharmacia LKB Biotechnology, Inc., Piscataway, NJ) or a TSK DEAE-5PW HPLC column (Pharmacia LKB Biotechnology, Inc.). DEAE columns were eluted with a 100–500 mM NaCl gradient in a buffer of 30 mM Tris-HCl, 0.5 mM DTT, pH 7.5, and peak fractions containing the 61-kD catalytic fragment of MLCK were pooled and further purified by hydroxylapatite chromatography (Ikebe et al., 1987a). The purified 61-kD fragment was concentrated to ~1 mg/ml, dialyzed against storage buffer, and stored at 4°C.

The extent and rate of  $\text{MLC}_{20}$  phosphorylation was assayed by incubating MLCK (10  $\mu\text{g/ml}$ ) or the 61-kD fragment (5  $\mu\text{g/ml}$ ) with 0.75 mg/ml gizzard myosin in a buffer of 150 mM NaCl, 25 mM Tris-HCl, 5 mM  $\text{MgCl}_2$ , 0.5 mM DTT, pH 7.5, containing either 0.2 mM  $\text{CaCl}_2$ /5  $\mu\text{g/ml}$  calmodulin or 1 mM EGTA (and 5  $\mu\text{g/ml}$  calmodulin in assays of MLCK). Reactions were initiated by the addition of ATP to 1 mM. 50- $\mu\text{l}$  aliquots of reaction mixtures were removed at various times, precipitated with 3–5% cold TCA, and washed with cold acetone prior to resuspension in urea-glycerol sample buffer (8.9 M urea, 30 mM Tris-glycine, 5 mM DTT, 0.2 mM EDTA, 0.01% bromophenol blue, pH 8.6). Samples were analyzed by urea-glycerol PAGE (Perrie and Perry, 1970) on 10% minislab gels stained with Coomassie blue, and quantified using an Ultrosan XL laser densitometer (Pharmacia LKB Biotechnology, Inc.).

Before injection into cells, MLCK and the 61-kD fragment were dialyzed into injection buffer (40 mM KCl, 20 mM Tris-HCl, 0.1 mM DTT, pH 7.0). The kinase activities were routinely assayed before and after microinjections. Inactive preparations of the 61-kD fragment were obtained by either dialyzing the active fragment for 24 h into a buffer of 10 mM Tris-acetate, 0.1 mM DTT, pH 7.0, or prolonged storage on ice for 10–14 d.

### Cell Culture, Microinjection, and Video Microscopy

NRK cells (NRK-52E; American Type Culture Collection, Rockville, MD) were cultured and plated for microinjection as previously described (Cao and Wang, 1990a). Microinjection dishes were cultured at 33°C on a microscope stage fitted with a completely enclosed incubator, which included encasement around the area of the microscope nosepiece to insure constant temperature regulation (McKenna and Wang, 1989). Prophase cells were identified by the appearance of condensing chromosomes and followed until nuclear envelope breakdown (NEB). Cells were microinjected ~5 min after NEB with a single pulse of solution, containing either; (a) injection buffer,

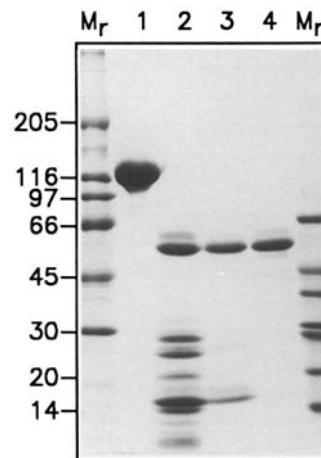
(b) MLCK at 1–4 mg/ml, (c) active 61-kD fragment at 0.5–2.0 mg/ml, or (d) inactive 61-kD fragment at 0.5–2.0 mg/ml. The pressure for microinjection was controlled with a custom-designed electronic pressure regulator.

The volume of microinjection was determined by a modified method of Lee (1989). Briefly, cells were injected with Lucifer yellow-labeled dextran (12 mg/ml; Molecular Probes, Inc., Eugene, OR) and fluorescence images were recorded with a cooled CCD camera (Star I; Photometrics, Tucson, AZ). The injected volume was then calculated based on the integrated fluorescence intensity over the whole cell. A standard curve was constructed by measuring total fluorescence intensities of microdroplets of 2.5 mg/ml Lucifer yellow-labeled dextran as a function of volume. Microdroplets were produced by spraying the fluorescent sample through an airbrush style nebulizer into a microinjection chamber filled with Type FF immersion oil (R. P. Cargille Laboratories, Inc., Cedar Grove, NJ). The volume of microinjection ranged from 0.01 to 0.03 pl. The volume of NRK cells, estimated by inducing cell rounding with trypsin and measuring the average diameter, is ~2.1 pl. Therefore, the volume of microinjection corresponded to 0.5–1.5% of the cell volume. Given the concentration of the protein solutions used for injection, we estimate the intracellular concentration of exogenous MLCK and 61-kD to be on the order of 0.05 to 0.5  $\mu\text{M}$ .

Phase contrast images were obtained with a Zeiss (Thornwood, NY) IM35 inverted microscope equipped with a 40 $\times$ /NA 0.65 achromat objective, and a low-light level ISIT video camera (Dage-MTI, Inc., Michigan City, IN). Images were stored as digital files in an image-processing computer, which was assembled by G. W. Hannaway and Associates (Boulder, CO) and consisted of a Silicon Graphics 4D/20 workstation (Mountain View, CA) and image-processing boards from Imaging Technology (150 series; Woburn, MA). Sequences of phase images were used to determine the timing of key stages of mitosis, and motile activities were analyzed using a motion display program as described previously (Wang, 1989).

### Fluorescence Localization of F-actin, Myosin, and Tubulin

Cells were followed for various periods of time before fixation. Cells stained for F-actin and myosin were fixed for 10 min with 3.2% formaldehyde (EM grade; Electron Microscopy Sciences, Fort Washington, PA) in PHEM buffer (60 mM Pipes, 25 mM Hepes, 10 mM EGTA, 2 mM  $\text{MgCl}_2$ , pH 6.1; Schliwa and van Blerkom, 1981), followed by a 5-min postfixation/extraction in acetone at -20°C. Samples were then blocked with PBS containing 1% BSA for ~30 min and reacted overnight at 4°C with a 1:20 dilution of an anti-myosin mAb (Klotz et al., 1986; Amac Inc., Westbrook, ME). Similar results were obtained with polyclonal anti-platelet myosin antibodies kindly provided by Drs. Ira Herman (Tufts University School of Medicine) and Keigi Fujiwara (National Cardiology Research Center, Osaka, Japan). After extensive washes with PBS/BSA, the samples were reacted with a 1:100 dilution of fluorescein conjugated sheep-anti-mouse secondary antibody (Sigma Chemical Corp., St Louis, MO). Cells were then stained with 0.2  $\mu\text{M}$  rhodamine phalloidin (Molecular Probes) for 45 min, washed with PBS, and examined by fluorescence microscopy. For microtubule staining,



205 kD, BSA; 45 kD, ovalbumin; 30 kD, carbonic anhydrase; 20 kD, soy bean trypsin inhibitor; 14 kD,  $\alpha$ -lactalbumin.

**Figure 1.** Preparation of the catalytic fragment of MLCK by limited tryptic digestion. Summary of the purification procedure by SDS-PAGE: lane 1, MLCK (7  $\mu\text{g}$ ); lane 2, digestion of MLCK with trypsin in the presence of  $\text{Ca}^{2+}$ /calmodulin; lane 3, pooled fraction from TSK DEAE-5PW HPLC; lane 4, 61-kD fragment after hydroxylapatite chromatography (3  $\mu\text{g}$ ). Molecular weight standards ( $M_r$ ) are in the far left and far right lanes, as indicated: 205 kD, myosin heavy chain; 116 kD,  $\beta$ -galactosidase; 97 kD, phosphorylase b; 66 kD, BSA; 45 kD, ovalbumin; 30 kD, carbonic anhydrase; 20 kD, soy bean trypsin inhibitor; 14 kD,  $\alpha$ -lactalbumin.

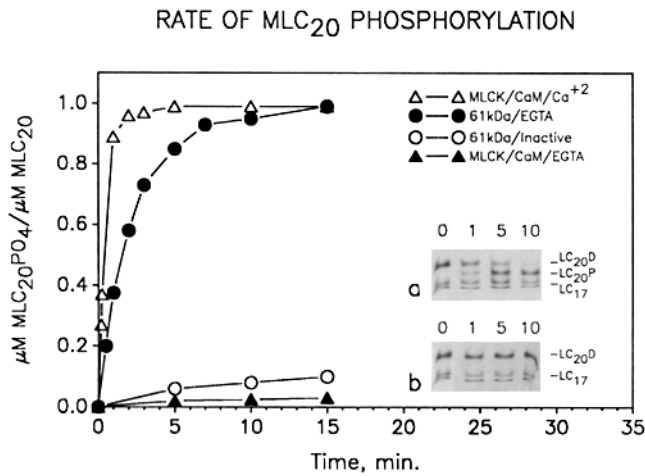


**Figure 2.** Phosphorylation activity of MLCK and the 61-kD catalytic fragment prepared for microinjection studies. MLC<sub>20</sub> is phosphorylated by MLCK in the presence of the Ca<sup>2+</sup>/calmodulin complex (*open triangles*), but not in the presence of EGTA and calmodulin (*closed triangles*). In contrast, the 61-kD catalytic fragment has a strong activity both in the presence of EGTA (*closed circles*) and in the presence of Ca<sup>2+</sup> (data not shown). After dialysis into a low ionic strength buffer or extended periods of storage on ice, the 61-kD fragment shows a greatly reduced activity (*open circles*). Gel insets show the urea-glycerol PAGE analysis of MLC<sub>20</sub> phosphorylation by an active 61-kD (*a*) and inactive 61-kD (*b*) preparation of the catalytic fragment of MLCK, at 0, 1, 5, and 10 min after the addition of ATP. LC<sub>20D</sub>, dephosphorylated MLC<sub>20</sub>; LC<sub>20P</sub>, phosphorylated MLC<sub>20</sub>; LC<sub>17</sub>, 17-kD myosin light chain. The band migrating slightly faster than LC<sub>17</sub> is most likely a proteolytic fragment of myosin.

cells were fixed for 10 min in 90% methanol, 50 mM EGTA, pH 6.0 at -15°C (Harris et al., 1980; Osborn and Weber, 1982), blocked, incubated with a 1:200 dilution of anti-β-tubulin mAb (Blose et al., 1984; Amersham Corp., Arlington Heights, IL), and stained as described above with fluorescent secondary antibodies. Fluorescence was observed with a Zeiss Axiovert-10 inverted microscope equipped with either a 100×/NA 1.3 Neofluar objective or infinity-corrected 100×/NA 1.3 Plan-Neofluar objective, using Zeiss 497715 and 497717 filter sets for rhodamine and fluorescein, respectively. Images were recorded and processed as previously described (McKenna et al., 1985).

### Other Procedures

Calmodulin was prepared from bovine brain according to Burgess et al. (1980) and smooth muscle myosin was prepared from turkey gizzard according to Ikebe and Hartshorne (1985). Protein concentrations were determined by the method of Lowry et al. (1951) using BSA as a standard. SDS-PAGE was performed according to Laemmli (1970) using 5–20% micro-slab gels (Matsudaira and Burgess, 1978), and Sigma SDS-6 and SDS-6H molecular weight standards.

**Table I.** Transit Times for Mitosis and Cytokinesis in Control and Microinjected Cells

	NEB to Anaphase onset (min)	Anaphase onset to midcytokinesis
Uninjected NRK cells	26.1 ± 3.9 (n = 19)	4.8 ± 0.8 (n = 15)
Active 61-kD fragment	46.6 ± 17.1 (n = 39)	4.9 ± 1.1 (n = 33)
Buffer-injected controls	28.1 ± 4.0 (n = 12)	4.6 ± 0.8 (n = 12)
Inactive 61-kD fragment	24.2 ± 4.1 (n = 7)	4.8 ± 0.9 (n = 28)
MLCK (Ca <sup>2+</sup> /CaM-dependent)	23.4 ± 4.3 (n = 13)	4.2 ± 1.3 (n = 10)

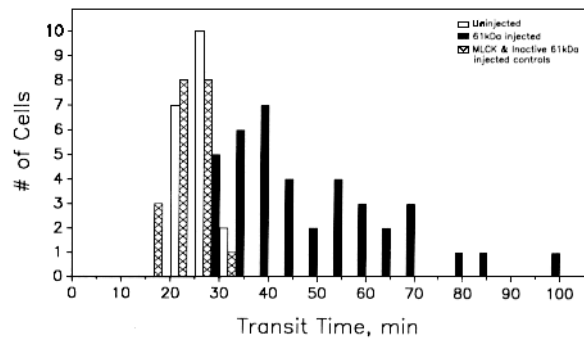


**Figure 3.** Frequency distribution of the transit time from NEB to anaphase onset for uninjected controls (*open bar*), inactive 61-kD fragment/MLCK injected controls (*crosshatched bar*), and active 61-kD fragment injected cells (*closed bar*). While the transit time for controls combined together is 25.6 ± 4.4 min, the transit time for cells injected with the active catalytic fragment of MLCK ranges from 25 to 97 min, with an average of 46.6 ± 17.1 min (also see Table I). Each bar represents the total number of cells within a 5-min time range, e.g., the solid bar at ~29 min on the abscissa represents five cells that had transit times ranging from 25 to 29 min.

## Results

### Biochemical Characterization of the 61-kD Catalytic Fragment of MLCK

MLCK is believed to be a highly specific enzyme that is stringently regulated by the binding interaction with the Ca<sup>2+</sup>/calmodulin complex. Using methods described by Ikebe et al. (1987a, 1989), we prepared a Ca<sup>2+</sup>/calmodulin-independent fragment of MLCK. As shown in Fig. 1, limited tryptic proteolysis of MLCK in the presence of Ca<sup>2+</sup> and calmodulin resulted in the cleavage of the protein into several well-defined fragments, from which a 61-kD fragment was purified using anion ion exchange and hydroxylapatite chromatography (Fig. 1, lane 4).

In biochemical assays, the 61-kD fragment caused rapid phosphorylation of MLC<sub>20</sub> independent of the presence of Ca<sup>2+</sup> and calmodulin (Fig. 2, *61kDa/EGTA*). However, because this activity was relatively short lived, showing a ~50% decrease within 7 d of the proteolytic cleavage of MLCK, microinjection experiments were performed within 5 d of preparation. Preparations of the 61-kD fragment that showed little or no catalytic activity in these assays (Fig. 2, *61kDa/inactive*) were used as controls in microinjection experiments described below.

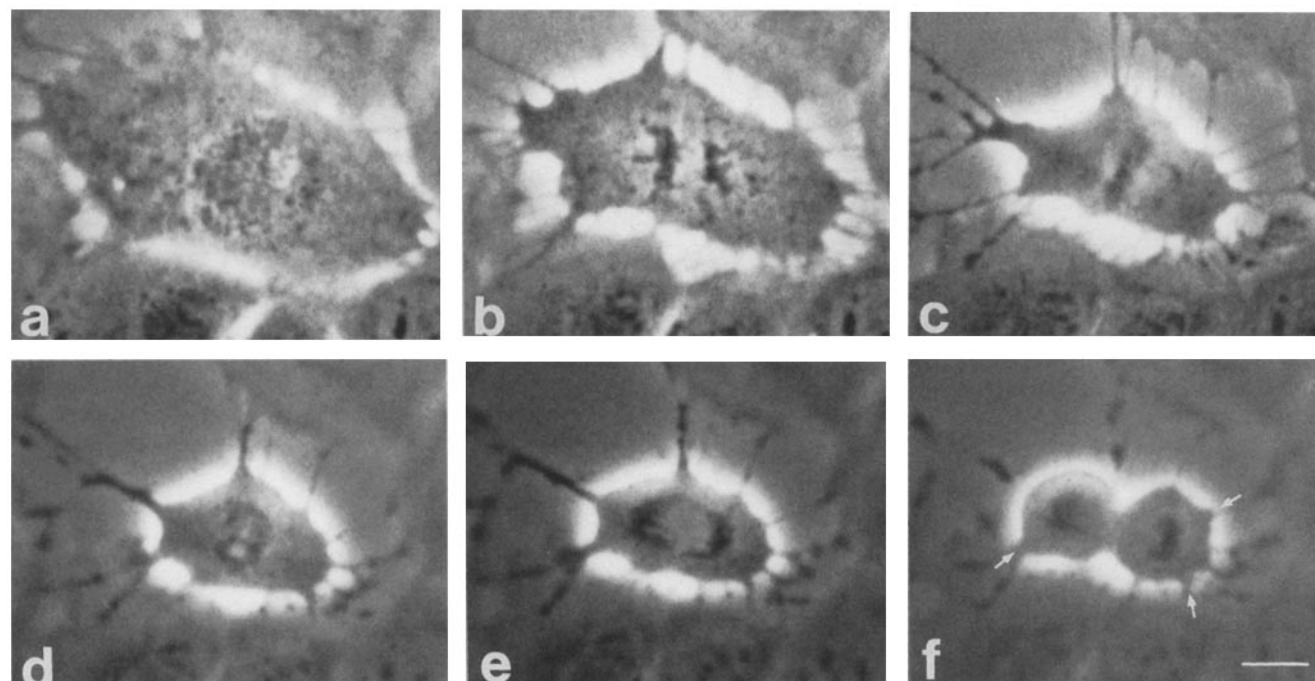


**Figure 4.** Time-lapse series of phase micrographs of a buffer-injected NRK cell during mitosis. After NEB (*a*,  $t = 0$  min), the cell was microinjected at  $t = 5$  min and observed through cell division. Images were recorded during prometaphase (*b*,  $t = 9.7$  min), metaphase (*c*,  $t = 19.4$  min), anaphase onset (*d*,  $t = 28.3$  min), anaphase II (*e*,  $t = 29.8$  min), and midcytokinesis (*f*,  $t = 32.2$  min). Note that the plasma membrane appears smooth around the cell, except for slender projections anchoring the cell to the substrate (*arrows*). Bar, 10  $\mu\text{m}$ .

#### **Microinjection of the 61-kD Catalytic Fragment of MLCK into Dividing Cells**

To define the timing of different stages of mitosis in NRK cells, we observed normal dividing cells by video microscopy and measured the period from NEB to midcytokinesis under conditions where the culture temperature was precisely maintained (see Materials and Methods). Uninjected cells showed a transit time from NEB to midcytokinesis averaging  $\sim 31$  min, with the period from NEB to anaphase onset lasting  $\sim 26$  min, and the period from anaphase onset to midcytokinesis lasting  $\sim 5$  min (Table I).

In contrast, cells injected with the active 61-kD fragment showed a significant delay in the progression through prometaphase and metaphase, with transit times between NEB and anaphase onset ranging from 25 to 97 min (Fig. 3; Table I). In addition,  $\sim 10\%$  of the injected cells failed to show normal karyokinesis or cytokinesis (see below). Surprisingly, all of the cells that completed karyokinesis showed no effect on the duration of anaphase or the rate of cytokinesis, as measured from the point of anaphase onset to midcytokinesis (Table I). Microinjection of cells with buffer alone, the inactive 61-kD fragment, or intact MLCK showed no effect on either the timing of mitosis or the rate of cytokinesis (Table I). Cells injected with control solutions exhibited typical morphological features of uninjected cells as they progressed through mitosis and cytokinesis, including chromosome condensation and NEB, chromosome congregation and alignment, chromosome separation, and formation of the cleavage furrow (Fig. 4).

In contrast, a large proportion (75%) of cells injected with the active 61-kD fragment showed striking surface blebbing

activities during later stages of mitosis. As shown in Fig. 5, the injected cell progressed through prometaphase with a normal phase morphology, however during anaphase highly active blebs showing rapid expansion and retraction activities were observed on the cell surface. The blebbing activity was initiated during metaphase in  $\sim 40\%$  of injected cells, and during anaphase in  $\sim 35\%$  of injected cells. Once started, the blebbing continued through the end of cell division. Blebs were initially observed over the entire surface during metaphase (Fig. 6), but as cells entered cytokinesis the blebbing activity subsided in the equatorial region where apparently normal cleavage furrows formed (Figs. 5 and 6). Upon completion of cytokinesis, the blebbing activity gradually decreased while daughter cells spread out in a manner similar to control cells. When 61-kD was injected during late metaphase and early anaphase, active blebbing was similarly observed in regions outside the equator, and there were no apparent effects on karyokinesis or the rate of cytokinesis (data not shown).

In a small percentage of injected cells that failed to show normal karyokinesis (mentioned above), metaphase chromosomes formed dispersed aggregates, while erratic blebs and constrictions were observed on the cell surface (Fig. 7, *a* and *b*). The failure to undergo normal cytokinesis was likely related to the abnormal karyokinesis observed in these cells.

#### **Fluorescence Localization of F-actin, Myosin, and Tubulin after Microinjection of the 61-kD Fragment**

The distribution of F-actin and myosin in cells microinjected with the 61-kD fragment was observed after staining with fluorescent phalloidin or specific antibodies against myosin.

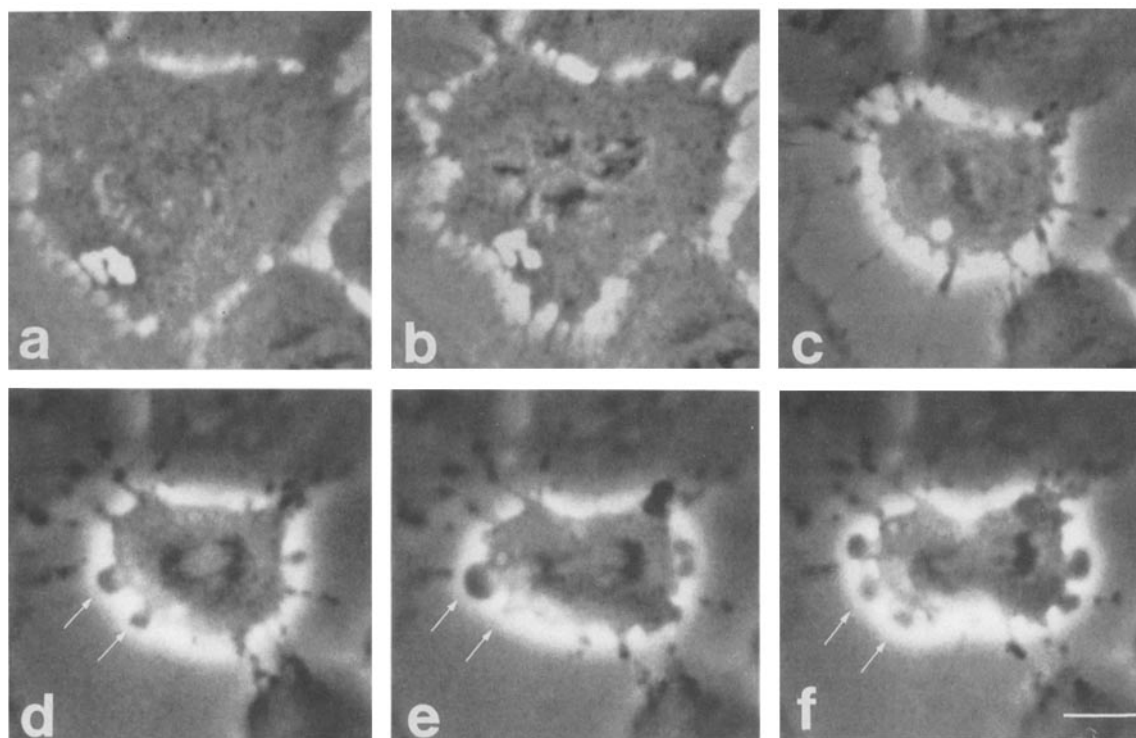


**Figure 5.** Time-lapse series of phase micrographs of a mitotic NRK cell injected with the 61-kD catalytic fragment of MLCK. After NEB (*a*,  $t = 0$  min), the cell was microinjected at  $t = 5$  min and followed through cell division. Although the phase morphology appears normal during prometaphase (*b*,  $t = 7.5$  min) and metaphase (*c*,  $t = 20.0$  min), blebbing activity initiates after the onset of anaphase (*d*,  $t = 26.9$  min) and continues through anaphase II (*e*,  $t = 28.4$  min) and cytokinesis (*f*,  $t = 29.4$  min). Note that the formation of the cleavage furrow at the equator is unaffected by the adjacent blebbing activity, and cytokinesis occurs at a rate similar to that for controls. Arrows indicate rapid extension and retraction of surface blebs. Bar,  $10\ \mu\text{m}$ .

In cells exhibiting dynamic surface activity, blebs were delineated by intense cortical staining of actin (Figs. 8 *a* and 9 *a*). In some cases actin and myosin were clearly localized near the base of the blebs (Fig. 9, *a* and *b*, arrows). In dividing cells both actin filaments and myosin were present in the cortex of the cleavage furrow, although the degree of staining varied from cell to cell as previously shown by others (Nunnally et al., 1980; Cao and Wang, 1990*a*). Similar distributions of actin and myosin in the furrow were observed for control cells and cells injected with the 61-kD fragment. Note that the variability of myosin staining in the furrow of

NRK cells was observed both with the monoclonal and polyclonal antibodies used in this study, however only the mAb appeared to show a distinct punctate staining pattern as previously observed in lymphoblasts (Bornens et al., 1989) and PtK<sub>2</sub> cells (Klotz et al., 1986).

To determine whether the delay of prometaphase and metaphase was related to disruptions of the mitotic spindle, injected cells were processed for immunofluorescence with anti-tubulin antibodies. Disrupted spindle structures, lacking well-defined kinetochore fibers, were observed in injected cells exhibiting prolonged periods of prometaphase

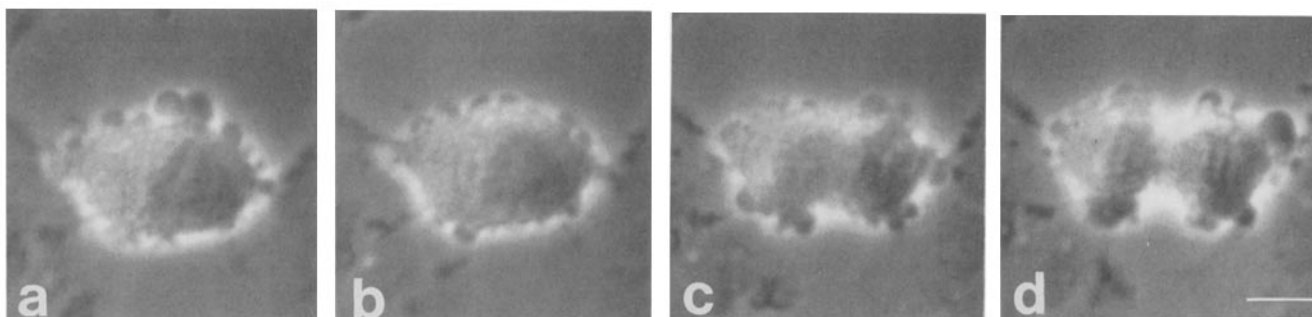


**Figure 6.** Time-lapse sequence of phase micrographs of a dividing NRK cell injected with the 61-kD catalytic fragment of MLCK. The cell was microinjected 5 min after NEB ( $t = 0$  min), and exhibited a significant delay in mitosis with a transit time from NEB to anaphase onset of 61.9 min. After an extensive period of metaphase blebbing (*a*,  $t = 60.1$  min), the surface activity subsided in the equatorial region during anaphase (*b*,  $t = 61.9$  min) and cytokinesis (*c*,  $t = 66.4$  min; and *d*,  $t = 67.6$  min). The cleavage furrow appears similar to that in control cells. Bar,  $10\ \mu\text{m}$ .

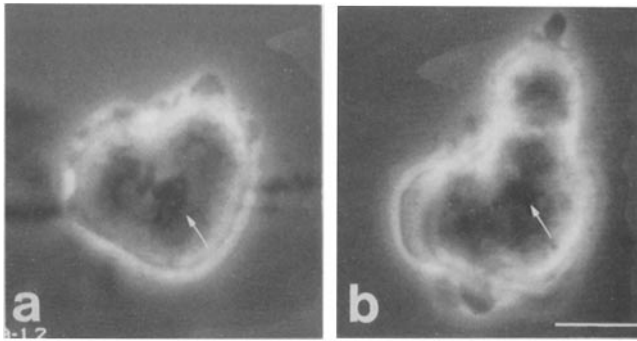


**Figure 7.** Phase contrast micrographs of two 61-kD injected cells that failed to undergo normal karyokinesis and cytokinesis. The cells were microinjected  $\sim 5$  min after NEB, and followed for 41 min (a) and 88 min (b), respectively. After prolonged periods in prometaphase/metaphase, the cells began to display abnormal surface activity resulting in constricted, multilobed phenotypes. These changes appeared to coincide with aborted attempts at karyokinesis as suggested by the dispersal and nonuniform segregation of phase-dense chromosomal material (arrows). Bar, 10  $\mu\text{m}$ .

and metaphase (Fig. 10, d and e). However, upon the onset of anaphase, the organization of spindle microtubules in 61-kD delayed cells (Fig. 10f) appeared similar to that of control cells (Fig. 10, g-i).

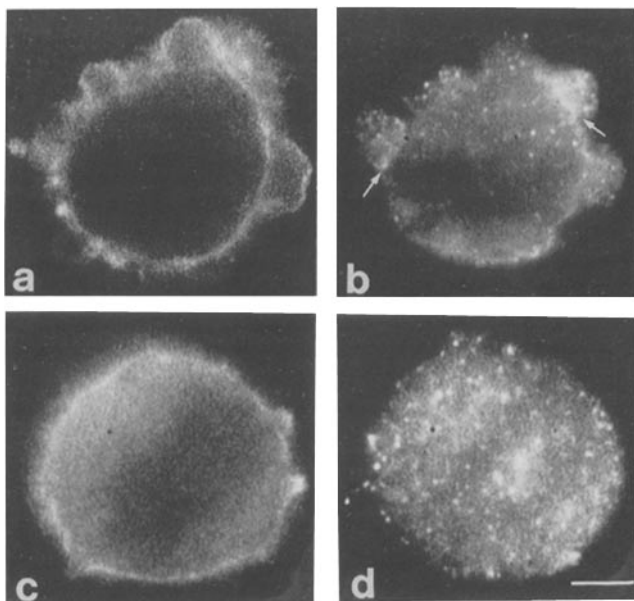


**Figure 8.** Distribution of F-actin and myosin in a mitotic NRK cell microinjected with the 61-kD fragment of MLCK and in an uninjected control cell. After injection of the 61-kD fragment at 5 min after NEB, the treated cell (a and b) displayed rapidly expanding and retracting surface blebs during metaphase. Both the injected cell and the control cell (c and d) were fixed at  $\sim 15$  min after NEB, which represents a typical time for metaphase in control cells, and stained for F-actin (a and c) and myosin (b and d). F-actin staining is localized on the cortex of the injected cell, while myosin staining is concentrated both on the cortex near the base of blebs (arrows) and as punctate foci in the cytoplasm. Similar results were obtained with polyclonal antibodies to myosin (see Materials and Methods), however only the mAb shows the distinct punctate staining pattern shown here (also see Fig. 9). Bar, 5  $\mu\text{m}$ .

## Discussion

Past biochemical studies have suggested a potentially important role for MLCK in regulating contractile activities in nonmuscle cells. The phosphorylation of the  $\text{MLC}_{20}$  at serine 19, after the activation of MLCK by  $\text{Ca}^{2+}$ -calmodulin complexes, could control both the assembly of myosin filaments and the generation of forces by actin-myosin interactions (Sellers and Adelstein, 1987). Thus it is possible that, during cell division, transient changes in the intracellular concentration of  $\text{Ca}^{2+}$  and/or the  $\text{Ca}^{2+}$ -calmodulin complex may regulate both spatially and temporally cortical contractile activities.

We sought to address this possibility by microinjecting the 61-kD constitutively active domain of MLCK. Such injections are expected to disturb the temporal and spatial regulations of the MLCK activity, and disrupt cellular functions that rely on the precise regulation of  $\text{MLC}_{20}$  phosphorylation. Two distinct effects, delays in the progression through prometaphase and metaphase, and surface blebbing activities during later stages of mitosis, were observed following the microinjections. Given the lack of effects after injections of buffer, intact MLCK, and inactive 61-kD fragment (Table I), the observed responses are likely due to the unregulated kinase activity of the 61-kD fragment, rather than nonspecific effects of the microinjection. The positive biological effects of the active catalytic fragment suggest that the activity of endogenous MLCK must be tightly regulated in dividing cells.

### Effects of the 61-kD Fragment on Cortical Activities

One of the most dramatic effects of the microinjection of the 61-kD fragment is the induction of active surface blebbing during metaphase and anaphase (Figs. 5 and 6). Although the mechanism for blebbing is poorly understood, it is likely that the 61-kD fragment causes an increase in the phosphorylation of myosin and stimulates contractile activities, which in turn may generate surface blebs through deformation of the cortical cytoskeleton and extrusion of the inner cytoplasm. This explanation is supported by the concentration of actin filaments and myosin in the cortex and near the base of blebs (Figs. 8 and 9; also see Herman et al., 1981, and Zelig and Wollman, 1977). In addition, a recent study has reported abnormal surface activities in *Dictyostelium* cells expressing a truncated myosin II, which lacks the ability to undergo disassembly and appears to show enhanced interactions with cortical actin (Egelhoff et al., 1991). Blebbing has also been observed in some transformed cell lines (Porter et al., 1973) and under conditions that presumably weaken the mechanical strength of the cortex, e.g., after the treatment of cells with cytochalasin B (Puck et al., 1972; Miranda et al., 1974; Perry and Snow, 1975; Godman and Miranda, 1978), or in melanoma cells deficient in the actin filament cross-linking protein filamin (Byers et al., 1991).

The apparent lack of blebbing during prometaphase in 61-kD-injected cells suggests that the activation of myosin-dependent motility may depend on multiple factors. For example, other kinases or phosphatases may affect the extent and/or sites of phosphorylation on  $\text{MLC}_{20}$  (Lamb et al., 1988; Fernandez et al., 1990). A particularly attractive possibility is that MLCK-dependent phosphorylation of  $\text{MLC}_{20}$  may be modulated by the activity of the  $\text{p34}^{\text{cdc}2}$  kinase (Sat-

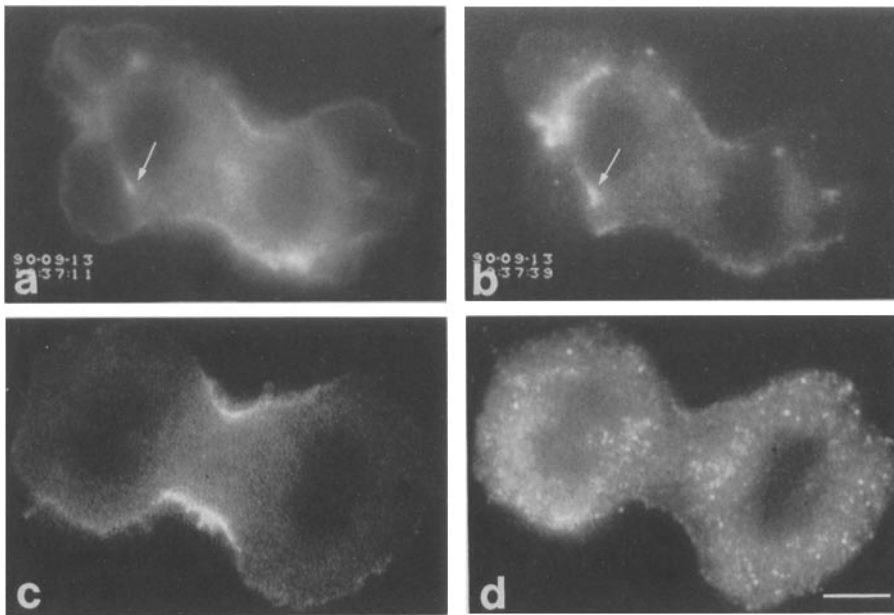


**Figure 9.** Distribution of F-actin and myosin during cytokinesis in a cell microinjected with the 61-kD fragment of MLCK and in an uninjected control cell. After injection of the 61-kD fragment at 5 min after NEB, the treated cell (*a* and *b*) displayed active surface blebs during metaphase and anaphase. Both the microinjected cell and the uninjected cell (*c* and *d*) were followed until midcytokinesis (~30 min after NEB for the injected cell), and fixed and stained for F-actin (*a* and *c*) and myosin (*b* and *d*). Actin is localized along the cortex and in the cleavage furrow of both 61-kD-injected and control cells, while myosin is present both on the cortex and in the cytoplasm. Note the intense staining of actin and myosin near the base of blebs in the microinjected cell (*a*, *b*; arrow). Bar, 5  $\mu$ m.

terwhite et al., 1990), which phosphorylates MLC<sub>20</sub> at serines 1, 2, and threonine 9, and inhibits MLCK-mediated phosphorylation of MLC<sub>20</sub> at serine 19 (Ikebe et al., 1987*b*; Sellers and Adelstein, 1987; Pollard et al. 1990). Thus, even though the 61-kD fragment is likely to be active during prometaphase, phosphorylation of MLC<sub>20</sub> at serine 19 may be inhibited until the activity of p34<sup>cdc2</sup> declines later in mitosis. Future studies to test the level and sites of MLC<sub>20</sub> phosphorylation in dividing cells will be extremely valuable.

### Effects of the 61-kD Fragment on Cytokinesis

Several mechanisms for the regulation of cytokinesis have been proposed (Rappaport, 1986; Salmon, 1989; Mabuchi, 1990; Pollard et al., 1990). One attractive hypothesis involves the preferential phosphorylation of myosin in the equatorial region by MLCK, presumably after the dephosphorylation of MLC<sub>20</sub> at the p34<sup>cdc2</sup> directed sites and a localized activation of MLCK by the Ca<sup>2+</sup>-calmodulin complexes (Pollard et al., 1990). The increase in the phosphory-

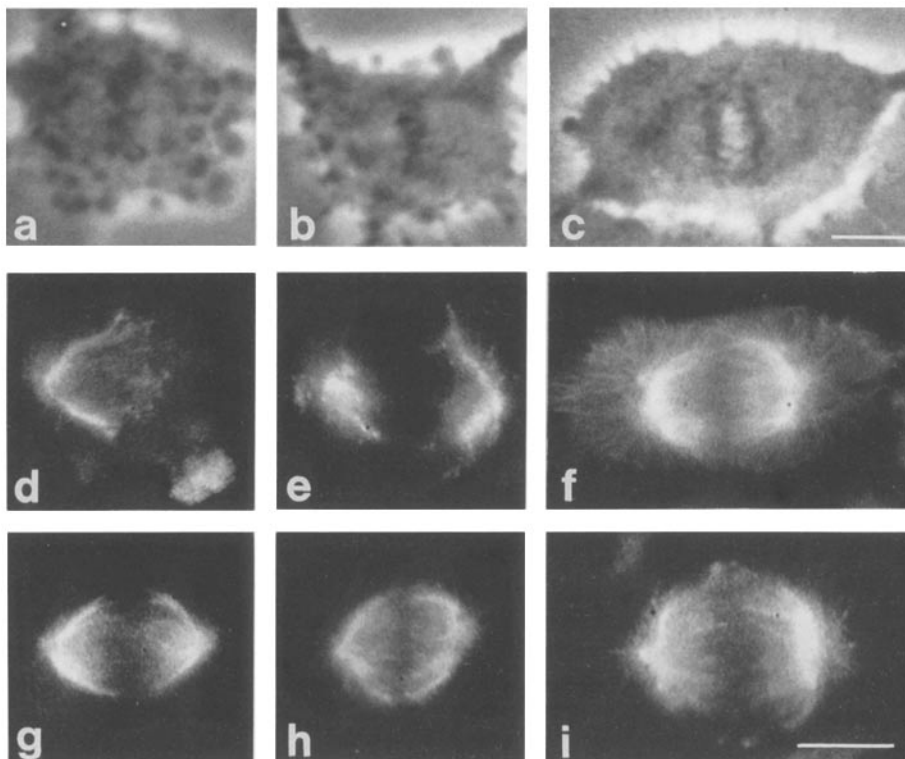


**Figure 10.** Distribution of tubulin in mitotic NRK cells microinjected with the 61-kD fragment and in uninjected control cells. Phase micrographs show three separate cells that were microinjected with the 61-kD fragment at 5 min after NEB and followed for 18 min (*a*), 26 min (*b*), and 45 min (*c*) before being fixed and stained with antibodies against tubulin. Corresponding fluorescence images indicate an apparent reduction or absence of kinetochore fibers in prometaphase/metaphase-delayed cells (*d* and *e*), but an apparently normal distribution of spindle microtubules in a cell at anaphase onset (*f*). Staining of control cells showed well-defined metaphase (*g* and *h*) and anaphase spindles (*i*). The more striking appearance of the spindle asters in *f* is likely due to the more fully spread shape of the cell. Magnification of phase images (*a-c*) are slightly lower than that of fluorescence images. Bars, 10  $\mu$ m.

lation of MLC<sub>20</sub> at serine 19 then activates contraction of the cleavage furrow. Based on this model, one would predict that changes in the degree, timing, or location of myosin phosphorylation could disrupt the process of cytokinesis. Specifically, microinjection of the 61-kD fragment should cause an unregulated phosphorylation of myosin throughout the entire cortex of dividing cells, that in turn might stimulate a global contraction and potentially disrupt both the timing and pattern of cell cleavage.

To our surprise, cytokinesis proceeded normally in the majority of 61-kD injected cells with respect to both the site and rate of cell cleavage (Figs. 5 and 6; Table I). These results indicate that additional factors, independent of the phosphorylation of MLC<sub>20</sub>, are likely involved in regulating cytokinesis. Based on previous studies, it is clear that cytokinesis involves not only acto-myosin interactions, but also formation of contractile structures in the cleavage furrow through the recruitment and organization of actin filaments and accessory proteins (Fujiwara et al., 1978; Aubin et al., 1979; Nunnally et al., 1980; Sanger et al., 1989; Cao and Wang, 1990a,b; Mabuchi, 1990; Pollard et al., 1990). Thus, the assembly of cross-linking proteins in the equatorial region may account for the suppression in blebbing activity concomitant with the organization of actin-myosin interactions into an effective cleavage force. In contrast, the lack of such organization in other regions may account for the sustained blebbing activities observed outside the furrow.

The regulation of cytokinesis may also involve the concerted activities of multiple kinases and phosphatases. While MLC<sub>20</sub> may be continually phosphorylated by the 61-kD catalytic fragment in injected cells, it is possible that only the equatorial region is able to maintain a specific pattern and level of phosphorylation during cytokinesis. The activity and localization of myosin in dividing cells may also be regulated by additional factors, such as phosphorylation of the heavy chains (Egelhoff et al., 1991), and/or association with myosin-binding proteins (Yabkowitz and Burgess, 1987). However, the physiological role of these factors in mammalian tissue culture cells remains to be elucidated.

### Effects of the 61-kD Fragment on Mitosis

One of the unexpected results of this study is that injection of the 61-kD catalytic fragment affects not only cortical activities, but also the progression of prometaphase and metaphase. Given the variety of evidence indicating that myosin II heavy chains are not directly involved in chromosome congression or segregation (Mabuchi and Okuno, 1977; Kiehart et al., 1982; De Lozanne and Spudich, 1987; Knecht and Loomis, 1987; Zurek et al., 1990), we are left with the question of how an increase in MLCK activity and elevation of phosphorylated MLC<sub>20</sub> might cause delays in mitosis.

The most direct explanation for such delays is that the dephosphorylation of MLC<sub>20</sub> at serine 19 is somehow required for the progression from metaphase to anaphase. This implies that MLC<sub>20</sub>, in addition to regulating myosin heavy chain activities, may also interact with other molecules involved in mitosis. One possibility is that, since MLC<sub>20</sub> can serve as a substrate for several kinases as well as phosphatases (Sellers and Adelstein), it is possible that increases in the phosphorylation state of MLC<sub>20</sub> may alter its interaction with these enzymes, resulting in a change in the balance of activities among different kinases and phosphatases involved in the

regulation of mitosis. Alternatively, the catalytic domain of MLCK is known to share some homology with other members of the Ca<sup>2+</sup>-calmodulin-dependent kinase family (Hanks et al., 1988; Olson et al., 1990; Shoemaker et al., 1990). Thus, the removal of certain noncatalytic domains during the preparation of 61-kD could affect its subcellular localization and/or substrate specificity, and cause delays in mitosis by phosphorylating proteins involved in spindle function. Finally, immunofluorescence studies suggest that MLCK may undergo redistribution from stress fibers in interphase cells (DeLanerolle et al., 1981) to kinetochore spindle-fibers in mitotic cells (Guerriero et al., 1981). This raises the question of whether MLCK may normally have additional substrates in the mitotic spindle, in addition to MLC<sub>20</sub>. Future experiments to test these ideas should yield new and important insights regarding the mechanism of mitosis and cytokinesis.

The authors would like to thank Drs. T. Keller, J. Sellers, T. Coleman, M. Ikebe, and Mr. M. Sanders for valued advice during the course of this work. In addition, we also extend special thanks to Drs. E. Luna and C. Wilkerson for help with HPLC procedures, Drs. G. Sluder and M. Melan for gifts of  $\beta$ -tubulin antibodies and advice on staining cells, and Bob's Turkey Farm (Clinton, MA) for generous donations of fresh gizzards. This project was supported by National Institutes of Health grant GM32476.

Received for publication 29 January 1991 and in revised form 28 May 1991.

### References

- Adelstein, R. S., and C. B. Klee. 1982. Purification of smooth muscle myosin light-chain kinase. *Methods Enzymol.* 85:298-308.
- Aubin, J. E., K. Weber, and M. Osborn. 1979. Analysis of actin and microfilament-associated proteins in the mitotic spindle and cleavage furrow of PtK2 cells by immunofluorescence microscopy. *Exp. Cell Res.* 124: 93-109.
- Blose, S. H., D. I. Meltzer, and J. R. Feramisco. 1984. 10nm filaments are induced to collapse in living cells microinjected with monoclonal and polyclonal antibodies against tubulin. *J. Cell Biol.* 98:847-858.
- Bornens, M., M. Paintrand, and C. Celati. 1989. The cortical microfilament system of lymphoblasts displays a periodic oscillatory activity in the absence of microtubules: implications for cell polarity. *J. Cell Biol.* 109:1071-1083.
- Burgess, W. H., D. K. Jemiolo, and R. H. Kretsinger. 1980. Interaction of calcium and calmodulin in the presence of sodium dodecyl sulfate. *Biochim. Biophys. Acta.* 623:257-270.
- Byers, H. R., T. Etoh, J. R. Doherty, A. J. Sober, and M. C. Mihm, Jr. 1991. Cell migration and actin organization in cultured human primary, recurrent cutaneous metastatic melanoma: time-lapse image analysis. *Am. J. Pathol.* 139:423-435.
- Cao, L.-G., and Y.-L. Wang. 1990a. Mechanism of the formation of contractile ring in dividing cultured animal cells. I. Recruitment of pre-existing actin filaments into the cleavage furrow. *J. Cell Biol.* 110:1089-1095.
- Cao, L.-G., and Y.-L. Wang. 1990b. Mechanism of the formation of contractile ring in dividing cultured animal cells. II. Cortical movement of microinjected actin filaments. *J. Cell Biol.* 111:1905-1911.
- De Lanerolle, P., R. S. Adelstein, J. R. Feramisco, and K. Burridge. 1981. Characterization of antibodies to smooth muscle myosin kinase and their use in localizing myosin kinase in nonmuscle cells. *Proc. Natl. Acad. Sci. USA.* 78:4738-4742.
- De Lozanne, A., and J. A. Spudich. 1987. Disruption of the *Dictyostelium* myosin heavy chain gene by homologous recombination. *Science (Wash. DC).* 236:1086-1091.
- Egelhoff, T. T., S. S. Brown, and J. A. Spudich. 1991. Spatial and temporal control of nonmuscle myosin localization: identification of a domain that is necessary for myosin filament disassembly in vivo. *J. Cell Biol.* 112: 677-688.
- Fernandez, A., D. L. Brautigan, M. Mumby, and N. J. C. Lamb. 1990. Protein phosphatase type-1, not type-2A, modulates actin microfilament integrity and myosin light chain phosphorylation in living nonmuscle cells. *J. Cell Biol.* 111:103-112.
- Fujiwara, K., and T. D. Pollard. 1976. Fluorescent antibody localization of myosin in the cytoplasm, cleavage furrow, and mitotic spindle of human cells. *J. Cell Biol.* 71:848-875.
- Fujiwara, K., and T. D. Pollard. 1978. Simultaneous localization of myosin and tubulin in human tissue culture cells by double antibody staining. *J. Cell*

- Biol.* 77:182-195.
- Fujiwara, K., M. E. Porter, and T. D. Pollard. 1978. Alpha-actinin localization in the cleavage furrow during cytokinesis. *J. Cell Biol.* 79:268-275.
- Godman, G. C., and A. F. Miranda. 1978. Cellular contractility and the visible effects of cytochalasin. In *Cytochalasins: Biochemical and Cell Biological Aspects*. S. W. Tanenbaum, editor. Elsevier/North Holland, Amsterdam. 277-429.
- Guerrero, V., Jr., D. R. Rowley, and A. R. Means. 1981. Production and characterization of an antibody to myosin light chain kinase and intracellular localization of the enzyme. *Cell.* 27:449-458.
- Hanks, S. K., Quinn, A. M., and T. Hunter. 1988. The protein kinase family: conserved features and deduced phylogeny of the catalytic domains. *Science (Wash. DC)*. 241:42-52.
- Harris, P., M. Osborn, and K. Weber. 1980. Distribution of tubulin-containing structures in the egg of the sea urchin *Strongylocentrotus purpuratus* from fertilization through first cleavage. *J. Cell Biol.* 84:668-679.
- Herman, I. M., N. J. Crisone, and T. P. Pollard. 1981. Relation between cell activity and the distribution of cytoplasmic actin and myosin. *J. Cell Biol.* 90:84-91.
- Ikebe, M., and D. J. Hartshorne. 1985. Effects of Ca<sup>2+</sup> on the conformation and enzymatic activity of smooth muscle myosin. *J. Biol. Chem.* 260:13146-13153.
- Ikebe, M., M. Stepinska, B. E. Kemp, A. R. Means, and D. J. Hartshorne. 1987a. Proteolysis of smooth muscle myosin light chain kinase. Formation of inactive and calmodulin-independent fragments. *J. Biol. Chem.* 260:13828-13834.
- Ikebe, M., D. J. Hartshorne, and M. Elzinga. 1987b. Phosphorylation of the 20,000-dalton light chain of smooth muscle myosin by the calcium-activated, phospholipid-dependent protein kinase. *J. Biol. Chem.* 262:9569-9573.
- Ikebe, M., S. Maruta, and S. Reardon. 1989. Location of the inhibitory region of smooth muscle myosin light chain kinase. *J. Biol. Chem.* 264:6967-6971.
- Itoh, T., M. Ikebe, G. J. Kargacin, D. J. Hartshorne, B. E. Kemp, and F. S. Fay. 1989. Effects of modulators of myosin light-chain kinase activity in single smooth muscle cells. *Nature (Lond.)*. 338:164-167.
- Kamm, K. E., and J. T. Stull. 1985. The function of myosin and myosin light chain kinase phosphorylation in smooth muscle. *Annu. Rev. Pharmacol. Toxicol.* 25:593-620.
- Kiehart, D. P., I. Mabuchi, and S. Inouye. 1982. Evidence that myosin does not contribute to force production in chromosome movement. *J. Cell Biol.* 94:165-178.
- Kitanishi-Yumura, T., and Y. Fukui. 1989. Actomyosin organization during cytokinesis: reversible translocation and differential redistribution in *Dicystostelium*. *Cell Motil. Cytoskeleton.* 12:78-89.
- Klotz, C., N. Bordes, M.-C. Laine, D. Sandoz, and M. Bornens. 1986. Myosin at the apical pole of ciliated epithelial cells as revealed by a monoclonal antibody. *J. Cell Biol.* 103:613-619.
- Knecht, D. A., and W. F. Loomis. 1987. Antisense RNA inactivation of myosin heavy chain gene expression in *Dicystostelium discoideum*. *Science (Wash. DC)*. 236:1081-1086.
- Korn, E. D., and J. A. Hammer, III. 1988. Myosins of nonmuscle cells. *Annu. Rev. Biophys. Biophys. Chem.* 17:23-45.
- Laemmli, U. K. 1970. Cleavage of structural proteins during the assembly of the head of bacteriophage T4. *Nature (Lond.)*. 227:680-685.
- Lamb, N. J. C., A. Fernandez, M. A. Conti, R. Adelstein, D. B. Glass, W. J. Welch, and J. R. Feramisco. 1988. Regulation of actin microfilament integrity in living nonmuscle cells by the cAMP-dependent protein kinase and the myosin light chain kinase. *J. Cell Biol.* 106:1955-1971.
- Lee, G. M. 1989. Measurement of volume injected into individual cells by quantitative fluorescence microscopy. *J. Cell Sci.* 94:443-447.
- Lowry, O. H., N. J. Rosebrough, A. L. Farr, and R. J. Randall. 1951. Protein measurement with the folin phenol reagent. *J. Biol. Chem.* 193:265-275.
- Mabuchi, I. 1986. Biochemical aspects of cytokinesis. *Int. Rev. Cytol.* 101:175-213.
- Mabuchi, I. 1990. Cleavage furrow formation and actin-modulating proteins. *Ann. NY Acad. Sci.* 582:131-146.
- Mabuchi, I., and M. Okuno. 1977. The effect of myosin antibody on the division of starfish blastomeres. *J. Cell Biol.* 74:251-263.
- Matsudaira, P. T., and D. R. Burgess. 1978. SDS micro-slab linear gradient polyacrylamide gel electrophoresis. *Anal. Biochem.* 87:386-396.
- Maupin, P., and T. D. Pollard. 1986. Arrangement of actin filaments and myosin-like filaments in the contractile ring and of actin-like filaments in the mitotic spindle of dividing HeLa cells. *J. Ultrastruct. Mol. Struct. Res.* 94:2-103.
- McKenna, N. C., and Y.-L. Wang. 1989. Culturing cells on the microscope stage. *Methods Cell Biol.* 29:195-205.
- McKenna, N. C., J. B. Meigs, and Y.-L. Wang. 1985. Exchangeability of alpha-actinin in living cardiac fibroblasts and myocytes. *J. Cell Biol.* 101:2223-2232.
- Miranda, A. F., G. C. Godman, and S. W. Tanenbaum. 1974. Action of cytochalasin D on cells of established lines. II. Cortex and microfilaments. *J. Cell Biol.* 62:406-423.
- Nunnally, M. H., J. M. D'Angelo, and S. W. Craig. 1980. Filamin concentration in cleavage furrow and mid-body region: frequency of occurrence compared with that of alpha-actinin and myosin. *J. Cell Biol.* 87:219-226.
- Olson, N. J., R. B. Pearson, D. S. Needleman, M. Y. Hurwitz, B. E. Kemp, and A. R. Means. 1990. Regulatory and structural motifs of chicken gizzard myosin light chain kinase. *Proc. Natl. Acad. Sci. USA.* 87:2284-2288.
- Osborn, M., and K. Weber. 1982. Immunofluorescence and immunocytochemical procedures with affinity purified antibodies: tubulin-containing structures. *Methods Cell Biol.* 24:97-132.
- Perrie, W. T., and S. V. Perry. 1970. An electrophoretic study of the low-molecular-weight components of myosin. *Biochem. J.* 119:31-38.
- Perry, M. M., and M. H. L. Snow. 1975. The blebbing response of 2-4 cell stage mouse embryos to cytochalasin B. *Dev. Biol.* 45:372-377.
- Pollard, T. D., L. Satterwhite, L. Cisek, J. Corden, M. Sato, and P. Maupin. 1990. Actin and myosin biochemistry in relation to cytokinesis. *Ann. NY Acad. Sci.* 582:120-130.
- Porter, K., D. Prescott, and J. Frye. 1973. Changes in surface morphology of chinese hamster ovary cells during the cell cycle. *J. Cell Biol.* 57:815-836.
- Puck, T. T., C. A. Waldren, and A. W. Hsie. 1972. Membrane dynamics in the action of dibutylryl adenosine 3':5'-cyclic monophosphate and testosterone on mammalian cells. *Proc. Natl. Acad. Sci. USA.* 69:1943-1947.
- Rappaport, R. 1986. Establishment of the mechanism of cytokinesis in animal cells. *Int. Rev. Cytol.* 105:245-281.
- Salmon, E. D. 1989. Cytokinesis in animal cells. *Curr. Op. Cell Biol.* 1:541-547.
- Sanger, J. M., B. Mittal, J. S. Dome, and J. W. Sanger. 1989. Analysis of cell division using fluorescently labeled actin and myosin in living PK2 cells. *Cell Motil. Cytoskeleton.* 14:201-219.
- Satterwhite, L., L. Cisek, J. Corden, and T. D. Pollard. 1990. A p34<sup>cdc2</sup>-containing kinase phosphorylates myosin regulatory light chain. *Ann. NY Acad. Sci.* 582:307.
- Sellers, J. R., and R. S. Adelstein. 1987. Regulation of contractile activity. In *The Enzymes*. P. D. Boyer and E. G. Krebs, editors. Academic Press, New York. Vol. 18. 381-418.
- Schliwa, M., and J. van Blerkom. 1981. Structural interaction of cytoskeletal components. *J. Cell Biol.* 90:222-235.
- Schroeder, T. 1987. Fourth cleavage of sea urchin blastomeres: microtubule patterns and myosin localization in equal and unequal cell divisions. *Dev. Biol.* 124:9-22.
- Shoemaker, M. O., W. Lau, R. L. Shattuck, A. P. Kwiatkowski, P. E. Matrisian, L. Guerra-Santos, E. Wilson, T. J. Lukas, L. J. Van Eldik, and D. M. Watterson. 1990. Use of DNA sequence and mutant analyses and antisense oligodeoxynucleotides to examine the molecular basis of nonmuscle myosin light chain kinase autoinhibition, calmodulin recognition, and activity. *J. Cell Biol.* 111:1107-1125.
- Walsh, M. P., S. Hinkins, R. Dabrowska, and D. J. Hartshorne. 1983. Smooth muscle myosin light chain kinase. *Methods Enzymol.* 99:279-288.
- Wang, Y.-L. 1989. Fluorescent analog cytochemistry: tracing functional protein components in living cells. *Methods Cell Biol.* 29:1-12.
- Warrick, H. M., and J. A. Spudich. 1987. Myosin structure and function in cell motility. *Annu. Rev. Cell Biol.* 3:379-421.
- Yabkowitz, R., and D. R. Burgess. 1987. Low ionic strength solubility of myosin in sea urchin egg extracts is mediated by a myosin-binding protein. *J. Cell Biol.* 105:927-936.
- Yumura, S., H. Mori, and Y. Fukui. 1984. Localization of actin and myosin for the study of amoeboid movement in *Dicystostelium* using improved immunofluorescence. *J. Cell Biol.* 99:894-899.
- Zeligs, J. D., and S. H. Wollman. 1977. Ultrastructure of blebbing and phagocytosis of blebs by hyperplastic thyroid epithelial cells in vivo. *J. Cell Biol.* 72:584-594.
- Zurek, B., J. M. Sanger, J. W. Sanger, and B. M. Jockusch. 1990. Differential effects of myosin-antibody complexes on contractile rings and circumferential belts in epitheloid cells. *J. Cell Sci.* 97:297-306.